CHAPTER II

PROPAGATING EHD INSTABILITIES IN NEMATICS

2.1 Introduction

The phenomenon of electrohydrodynamic (EHD) instabilities in nematic liquid crystals (NLC) has been discussed in some detail in Chapter I of this thesis. NLCs with negative or weakly positive dielectric anisotropy ($\Delta\epsilon$) give rise to convective instabilities in the form of cylindrical rolls or domains under the action of a DC or AC electric voltage above a threshold value. Due to the simplicity of the experimental set-up this dissipative system has gained importance in the study of pattern formation [Lowe and Gollub, 1985; Rehberg et al., 1988].

In recent years, a travelling wave (TW) instability has been observed in the conduction regime, especially in thin samples at frequencies at which either normal or oblique rolls occur (Rehberg *et al.*, 1388, 1989). In this type of instability the pattern moves parallel to the wavevector with equal probability of taking either of the two possible directions. However so far all the theoretical studies have failed to obtain solutions corresponding to such a TW mode.

The possibility of either oscillatory or TW electroconvection in nematics under

DC excitation has been discussed in the past by a few authors. Ioffe (1975) included the flexoelectric terms in EHD equations and incorrectly got oscillatory solutions, because the flexoelectric terms used in the equations of motion and in the torque balance equations were incorrect (see later discussion). Matyushichev and Kovnatskii (1975) have also got incorrect oscillatory solutions because the boundary conditions were not properly taken into account. Laidlaw (1979) using an analogy with the oscillatory instability predicted by Lekkerkerker (1978) for thermal convection, showed that materials with *positive* dielectric anisotropy and *negative* conductivity anisotropy could, in principle, exhibit an oscillatory EHD instability under a DC field. But this has not been experimentally observed since the threshold for this instability is much higher than that for the Freedericksz transition. Penz (1975) suggested that in materials with positive $\Delta\epsilon$ and positive $\Delta\sigma$, a TW EHD instability can set in if the sample thickness is very small, but again at DC voltages above the Freedericksz threshold.

In the following, we present theoretical calculations in which we extend Penz's treatment by including flexoelectric terms. We find that the flexoelectric contribution suppresses the travelling wave solutions found by Penz. In all these theoretical calculations, it is presumed that the NLC is homogeneously aligned, with its director making zero pretilt angle at the cell walls. However, we find that if the symmetry of the cell is changed by having a small pretilt angle at the cell boundaries, a *propagating EHD* instability results at the threshold of DC excitation due to some additional flexoelectric torques which are $\pi/2$ radians out of phase with the main torques responsible for EHD instability. We present a simple one-dimensional model which itself brings out this result. We also present a detailed two dimensional model in which the proper boundary conditions are included, which essentially confirms the

results of the 1D model. As flexoelectric effect provides the driving mechanism for this propagating mode, the direction of propagation reverses when the applied field is reversed. We also present an experimental study which confirms this prediction of the theory.

2.2 Travelling Wave (TW) Instability

As was mentioned earlier, Penz (1975) obtained for an applied DC field oscillatory solutions of the EHD equations, for materials with positive dielectric and conductivity anisotropies. Such solutions exist only at voltages above the Freedericksz threshold and only for very thin samples. Penz had not included flexoelectric terms in his analysis. We were interested to check if the latter terms give rise to TW solutions for negative $\Delta\epsilon$ materials. Hence we have extended Penz's model by including the flexoelectric terms.

Penz solved the problem by considering the proper boundary conditions. As we are interested in finding threshold contlitions, at which the amplitudes are expected to be very small, we linearise the equations. The linearised EHD equations describing such a system, can be written as follows (see Chapter I).

1) *Poisson equation*

$$4\pi Q - \epsilon_{\parallel}\frac{\partial E_x}{\partial x} - \epsilon_{\perp}\frac{\partial E_z}{\partial z} - \Delta\epsilon E_o\frac{\partial\theta}{\partial x} - 4\pi(e_1 + e_3)\frac{\partial^2\theta}{\partial x\partial z} = 0 \qquad (2.1)$$

where e_1 and e_3 are the flexoelectric coefficients.

2) Charge conservation equation

$$\frac{\partial Q}{\partial t} + \sigma_{\parallel}\frac{\partial E_x}{\partial x} + \sigma_{\perp}\frac{\partial E_z}{\partial z} + \Delta\sigma E_o\frac{\partial\theta}{\partial x} = 0 \qquad (2.2)$$

3) *Torque balance equation*

$$\gamma_1 \frac{\partial \theta}{\partial t} - K_3 \frac{\partial^2 \theta}{\partial x^2} - K_1 \frac{\partial^2 \theta}{\partial z^2} - \frac{\Delta \epsilon}{4\pi}[E_o^2 \theta + E_o E_x] + (e_1 + e_3)\frac{\partial E_x}{\partial z} + \alpha_3 \frac{\partial v_x}{\partial z} + \alpha_2 \frac{\partial v_z}{\partial x} = 0 \tag{2.3}$$

where K_1 and K_3 are splay and bend elastic constants, and $\gamma_1 = (\alpha_3 - \alpha_2)$ where a; are the Leslie viscosity coefficients.

4) *Equations of motion*

$$-\frac{\partial P}{\partial x} + \alpha_3 \frac{\partial^2 \theta}{\partial z \partial t} + \eta_1 \frac{\partial^2 v_x}{\partial x^2} + \eta_2 \frac{\partial^2 v_x}{\partial z^2} = 0 \tag{2.4}$$

and

$$-\frac{\partial P}{\partial z} + \alpha_2 \frac{\partial^2 \theta}{\partial x \partial t} + \eta_3 \frac{\partial^2 v_z}{\partial z^2} + \eta_4 \frac{\partial^2 v_z}{\partial x^2} + E_o Q = 0 \tag{2.5}$$

where P is the pressure, $\eta_1 = \alpha_1 + \alpha_5 + \frac{1}{2}(\alpha_4 + \alpha_3 + \alpha_6)$, $\eta_2 = \frac{\alpha_3 + \alpha_4 + \alpha_6}{2}$, $\eta_3 = \frac{\alpha_4 - \alpha_5 - \alpha_2}{2}$ and $\eta_4 = \frac{\alpha_4 + \alpha_5 - \alpha_2}{2}$

We use the method of Penz and Ford (1972) to solve these equations. We assume solutions of the form,

$$\begin{aligned} Q &= Q_1 e^{i(\vec{q}\cdot\vec{r} - \omega t)}; \quad v_z = v_1 e^{i(\vec{q}\cdot\vec{r} - \omega t)}; \quad v_x = -S v_1 e^{i(\vec{q}\cdot\vec{r} - \omega t)}; \\ E_x &= E_1 e^{i(\vec{q}\cdot\vec{r} - \omega t)}; \quad E_z = S E_1 e^{i(\vec{q}\cdot\vec{r} - \omega t)}; \quad \theta = \theta_1 e^{i(\vec{q}\cdot\vec{r} - \omega t)}; \\ P &= P_1 e^{i(\vec{q}\cdot\vec{r} - \omega t)} \end{aligned} \tag{2.6}$$

where $w = w_r - i\omega_i$, and $S = q_z/q_x$. In deriving equation (2.6) we have used the continuity equation

$$\frac{\partial v_x}{\partial x} + \frac{\partial v_z}{\partial z} = 0 \tag{2.7}$$

and the Maxwell equation

$$\frac{\partial E_x}{\partial z} - \frac{\partial E_z}{\partial x}. \tag{2.8}$$

Using the solutions (eqn.2.6) in the EHD equations (2.1) to (2.5), the following simplified amplitude equations are obtained.

a) After eliminating Q using Poisson equation, the charge conservation equation becomes

$$\frac{1}{q_x}\left[(\sigma_{\|}+\sigma_{\perp}S^2) - \frac{i\omega}{4\pi}(\epsilon_{\|}+\epsilon_{\perp}S^2)\right]E_1 + \left[\Delta\sigma U - \frac{i\omega\Delta\epsilon U}{4\pi} + \omega(e_1+e_3)S\right]\theta_1 = 0 \qquad (2.9)$$

where $U = E_o/q_x$.

b) Torque balance equation

$$i(\alpha_2-\alpha_3S^2)v_1 - \left[\frac{\Delta\epsilon}{4\pi}U - i(e_1+e_3)S\right]E_1 + q_x\left(K_3+K_1S^2-\frac{\Delta\epsilon}{4\pi}U^2 - i\gamma_1\frac{\omega}{q_x^2}\right)\theta_1 = 0 \qquad (2.10)$$

c) The x-component of equation of motion,

$$-\frac{iP_1}{q_x} + (\eta_1+\eta_2S^2)Sv_1 + \frac{\alpha_3\omega S}{q_x}\theta_1 = 0 \qquad (2.11)$$

d) The z-component of equation of motion,

$$-\frac{iSP_1}{q_x} + (\eta_4+\eta_3S^2)v_1 + \frac{iU}{4\pi}(\epsilon_{\|}+\epsilon_{\perp}S^2)E_1 + \left[\frac{\alpha_2\omega}{q_x} + \frac{Uq_x}{4\pi}(i\Delta\epsilon U - 4\pi(e_1+e_3)S)\right]\theta_1 = 0 \qquad (2.12)$$

Equations (2.9) to (2.12) form a set of homogeneous equations in the variables P_1, v_1, E_1 and θ_1. For the existence of non-trivial solutions the determinant of the coefficients of the variables in tlie above equations should vanish. This condition yields the following 8th degree polynomial in S

$$\sum_{j=0}^{8} a_j S^j = 0 \qquad (2.13)$$

The coefficients of the polynomial are :

$$a_o = \frac{U^2}{4\pi}(\alpha_2 P + \eta_5 \Delta\epsilon\Delta\sigma) + \eta_5\sigma_{||}L + \frac{\beta_2\epsilon_{||}\omega^2}{4\pi q_x^2}$$

$$+i\omega\left[-\eta_5(\frac{\Delta\epsilon U}{4\pi})^2 + \frac{\beta_2\sigma_{||}}{q_x^2} - \frac{\eta_5\epsilon_{||}L}{4\pi}\right]$$

$$a_1 = [-i(e_1+e_3)U(\alpha_2\sigma_{||} + \eta_5\Delta\sigma)]$$

$$a_2 = \left[\eta_6\frac{\Delta\epsilon\Delta\sigma U^2}{4\pi} + M_2L - \frac{M_4\gamma_1\omega^2}{4\pi q_x^2} + \frac{\omega^2}{4\pi q_x^2}(\alpha_2^2\epsilon_\perp - 2\alpha_2\alpha_3\epsilon_{||})\right.$$

$$\left.+\eta_5 K_1\sigma_{||} + \frac{U^2P}{4\pi}(\alpha_2-\alpha_3)\right] + i\omega\left[-\eta_6\left\{\left(\frac{\Delta\epsilon U}{4\pi}\right)^2 + \frac{\gamma_1\sigma_{||}}{q_x^2}\right\} - \frac{M_4L}{4\pi}\right.$$

$$\left.-\frac{2\alpha_2\alpha_3\sigma_{||}}{q_x^2} - \eta_5\left\{(e_1+e_3)^2 + \frac{K_1\epsilon_{||}}{4\pi}\right\} + \frac{\beta_2\sigma_\perp}{q_x^2}\right]$$

$$a_3 = [i(e_1+e_3)U(-\eta_6\Delta\sigma + \alpha_3\sigma_{||} - \alpha_2\sigma_\perp)]$$

$$a_4 = \left[M_2K_1 + M_1L - \frac{\omega^2}{4\pi q_x^2}\left\{(\eta_6\gamma_1 + 2\alpha_2\alpha_3)\epsilon_\perp - \beta_1\epsilon_{||}\right\}\right.$$

$$+\frac{U^2}{4\pi}(\eta_3\Delta\epsilon\Delta\sigma - \alpha_3P) + i\omega\left\{-\eta_6(e_1+e_3)^2 - \frac{M_4K_1}{4\pi}\right.$$

$$\left.\left.-\frac{\sigma_\perp}{q_x^2}(\eta_6\gamma_1 + 2\alpha_2\alpha_3) - \frac{M_3L}{4\pi} + \frac{\beta_1\sigma_{||}}{q_x^2} - \eta_3\left(\frac{\Delta\epsilon U}{4\pi}\right)^2\right\}\right]$$

$$a_5 = [i(e_1+e_3)U(-\eta_3\Delta\sigma + \alpha_3\sigma_\perp)]$$

$$a_6 = \left[M_1 K_1 + \eta_3 \sigma_\perp L + \frac{\beta_1 \epsilon_\perp \omega^2}{4\pi q_x^2} + i\omega\left\{-\frac{M_3 K_1}{4\pi} - \eta_3 (e_1 + e_3)^2 + \frac{\beta_1 \sigma_\perp}{q_x^2} - \frac{\eta_3 \epsilon_\perp L}{4\pi}\right\}\right]$$

$$a_8 = \left[\eta_3 K_1 \sigma_\perp - \frac{i\omega \eta_3 K_1 \epsilon_\perp}{4\pi}\right]$$

where $\eta_5 = \frac{1}{2}(\alpha_4 + \alpha_5 - \alpha_2)$; $\eta_6 = \eta_1 - \eta_2 - \eta_4 + \alpha_4$; $M_1 = \eta_6 \sigma_\perp + \eta_3 \sigma_\parallel$;
$M_2 = \eta_6 \sigma_\parallel + \eta_5 \sigma_\perp$; $M_3 = \eta_6 \epsilon_\perp + \eta_3 \epsilon_\parallel$;, $M_4 = \eta_6 \epsilon_\parallel + \eta_5 \epsilon_\perp$; $L = K_3 - \frac{AcU^2}{4\pi}$;
$P = \epsilon_\parallel \Delta\sigma - \Delta\epsilon \sigma_\parallel = \epsilon_\perp \Delta\sigma - \Delta\epsilon \sigma_\perp$; $\beta_1 = \alpha_3^2 - \eta_3 \gamma_1$; $\beta_2 = \alpha_2^2 - \eta_5 \gamma_1$

Since equation *(2.13)* is of the eighth order in S, there are eight possible solutions for S and the general solutions can be written as, for e.g.,

$$\theta = \sum_{j=1}^{8} \theta_j e^{i[q_x(x + S_j z) - \omega t]} \tag{2.13a}$$

and

$$v_x = -\sum_{j=1}^{8} S_j v_j e^{i(q_x(x + S_j z) - \omega t)} \tag{2.13b}$$

Similar expressions can be written for the other variables. These general solutions for the variables should also satisfy the following boundary conditions at the two surfaces of the cell. Assuming strong anchoring at the plates,

$$\theta(z = \pm d/2) = 0 \tag{2.14a}$$

Since the plates are conducting, the transverse field $E_x = 0$ at the plates. Hence

$$E_x(z = \pm d/2) = 0 \tag{2.14b}$$

As there is no flow at the plates, it follows that

$$v_x(z = \pm d/2) = 0 \tag{2.14c}$$

and

$$v_z(z = \pm d/2) = 0 \tag{2.14d}$$

The two boundary conditions at $z = \pm d/2$ on v_z lead to the following equations

$$\sum_{j=1}^{8} v_j e^{iS_j\delta} e^{-i\omega t} = 0 \tag{2.15}$$

where $6 = q_x d/2$, and

$$\sum_{j=1}^{8} v_j e^{-iS_j\delta} e^{-i\omega t} = 0 \tag{2.16}$$

where v_j are arbitrary coefficients. On adding the equations (2.15) and (2.16) we get,

$$\sum_{j=1}^{8} v_j \sin S_j\delta = 0 \tag{2.17}$$

and

$$\sum_{j=1}^{8} v_j \cos S_j\delta = 0 \tag{2.18}$$

The other boundary conditions lead to similar equations for other variables. They can be written in terms of the coefficients v_j making use of the equations (2.9) to (2.12). Then we get a set of 8 linear equations in v_j. For the existence of solutions satisfying the boundary conditions the determinant of coefficients associated with these equations should also vanish. This boundary value determinant can be symbolically written as

$$D_{ij} = 0; \quad i, j = 1, 8 \tag{2.19}$$

Equations (2.13) and (2.19) form a characteristic value problem and any arbitrary set of roots of equation (2.13) will not, in general, satisfy equation (2.19). Therefore in order to obtain the solutions, we have to find a set of values of S_j that satisfy both these equations simultaneously. The calculations are made numerically. For a given set of values of the material parameters and a given value of w, we choose

some values of the applied voltage V_a and 6 and tlie roots of euation (2.13) arc obtained. These roots are then substituted in equation (2.19), and the boundary value determinant (BVD) is evaluated. The value of 6 is varied till BVD reduces to zero. The calculations are repeated for different values of the voltage. Then the lowest value of the voltage at which such solutions exist is the threshold voltage V_{th}, and the corresponding value of 6 gives the magnitude of the wavevector q. The above process is then repeated for a different value of w. Thus for applied fields greater than or equal to a threshold value (V_{th}), the boundary value problem can be satisfied only for particular values of w and $q_x(\delta)$.

In order to locate the range of existence of solutions corresponding to travelling wave instability Penz (1975) used a simple method. He took tlie real part of w (i.e., w_r) $= 0$ and calculated for each value of q, that value of ω_i (the imaginary part of w), which satisfies the EHD equations, along with the boundary conditions. For voltages above the Freedericksz Transition Voltage he found the variation of ω_i versus q_x as shown in figure 2.1 which is plotted for a $1\mu m$ thin MBBA sample at an applied voltage of 2.8 V. A gap is found in the graph for which no solutions are found (Fig.2.1).

However solutions to EHD equations can be found in this gap when $\omega_r \neq 0$. This implies that the solutions in this region arc not stationary. The variation of ω_i as a function of ω_r in this gap, for which the boundary value problem is solved with q_x as a parameter, is plotted in figure 2.2. The particular value of tlie voltage used in the calculations is the threshold voltage for the instability when $\omega_i = 0$. Since w_r is noti-zero this threshold is for a TW EIID instability, which travels with a velocity of ω_r/q_x.

As we described earlier, we have included the flexoelectric contribution (equa-

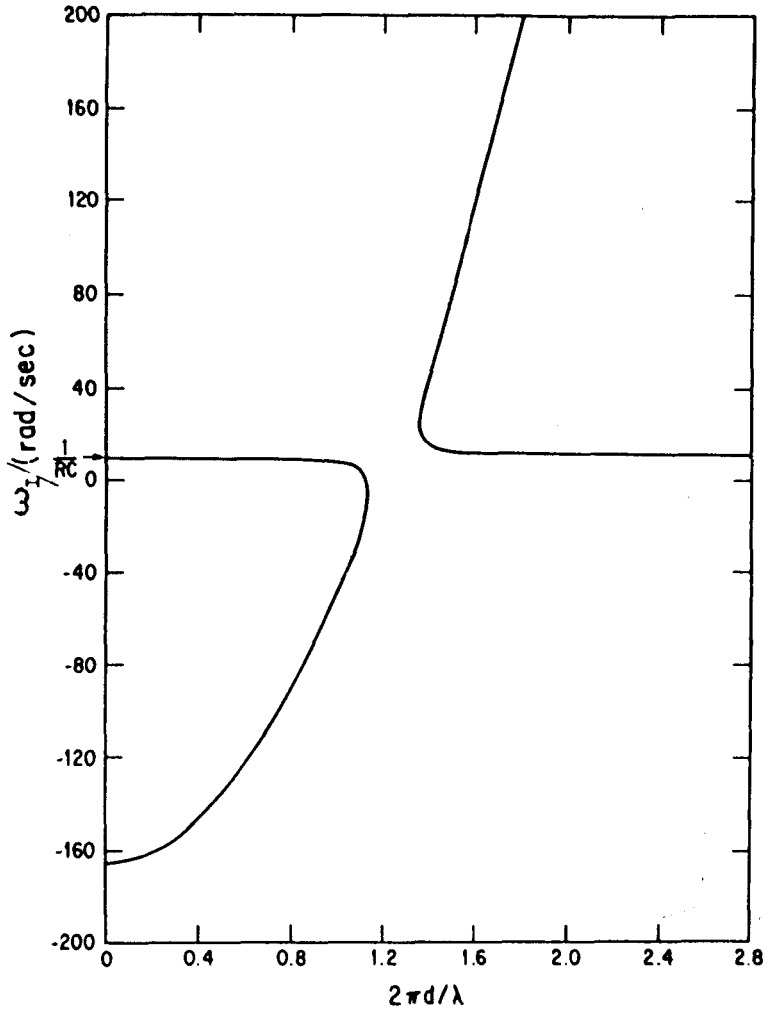

Fig.2.1: Dispersion relation for a 1 μm thick sample of MBBA. For all the solutions of ω_i vs. $2\pi d/\lambda$ shown in the graph, ω_r=0. The gap in solutious indicate that an oscillatory time-dependence is necessary to solve the boundary value problem in this gap (Ref. Penz, 1975).

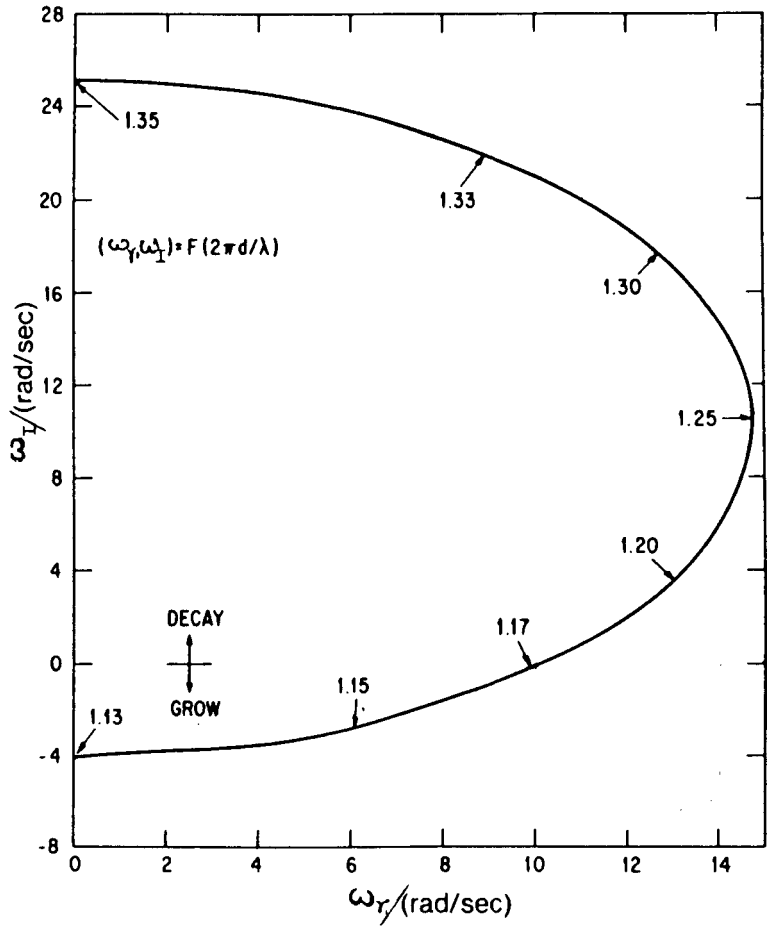

Fig.2.2: The complex frequencies (w_r, ω_i) of modes in the gap shown in Fig.2.1 are plotted as functions of the normalised wavevector. At $2\pi d/\lambda$=1.17, ω_i=0 and ω_r=10 rad/sec. Under these conditions a distortion will freely propagate with a velocity of $8.5\times10^{-6}.m/sec$ in a 1 μm thick sample (Itef. Penz, 1975).

tions 2.1-2.5) to the EHD equations to study its influence on the TW mode. The results of our calculations are shown in figure **2.3.** The above calculations have been made using the physical parameters of MBBA listed in table 2.1, except $\Delta\epsilon$ which is assumed to be positive.

From figure **2.3** it is clear that the flexoelectric contribution reduces the width of the gap in which TW instability occurs. As the magnitude of the flexoelectric terrn $(e_1 + e_3)$ is increasecl, the gap width is progressively reduced. Thus tlie flexoelectric contribution actually suppresses the TW EHD instability. We have also confirmed that when $\Delta\epsilon = 0$ or negative, there is no TW solutions to the EHD equation even when the flexoelectric contribution is incorporated.

2.3 Propagating EHD Instability - One-Dimensional Treatment

It is now well established that the technique of rubbing polyimide coated glass plates to align a nematic liquid crystal results in a small pre-tilt angle of tlie director at the bounding plates (Mosley ***et al.,*** 1987). In the following we study the EHD instability in nematic liquid crystals aligned with such a pretilt angle at tlie surfaces. The plates are assumed to be in a mutually antiparallel orientation so that the nematic director $\hat{n}$ is aligned with a constant pretilt angle (β) throughout the cell. We show that in such a cell, at the threshold of DC excitation, flexoelectric torques which are $\pi/2$ radians out of phase with the torques produced due to other mechanisms come into play. As a consequence of these out of phase torques, the EHD pattern slowly propagates normal to the roll axis and in a direction which depends on the sign of the applied field E,, the tilt angle (β) and the sign of the combination $(e_1 + e_3)$ of tlie flexoelcctric coefficients.

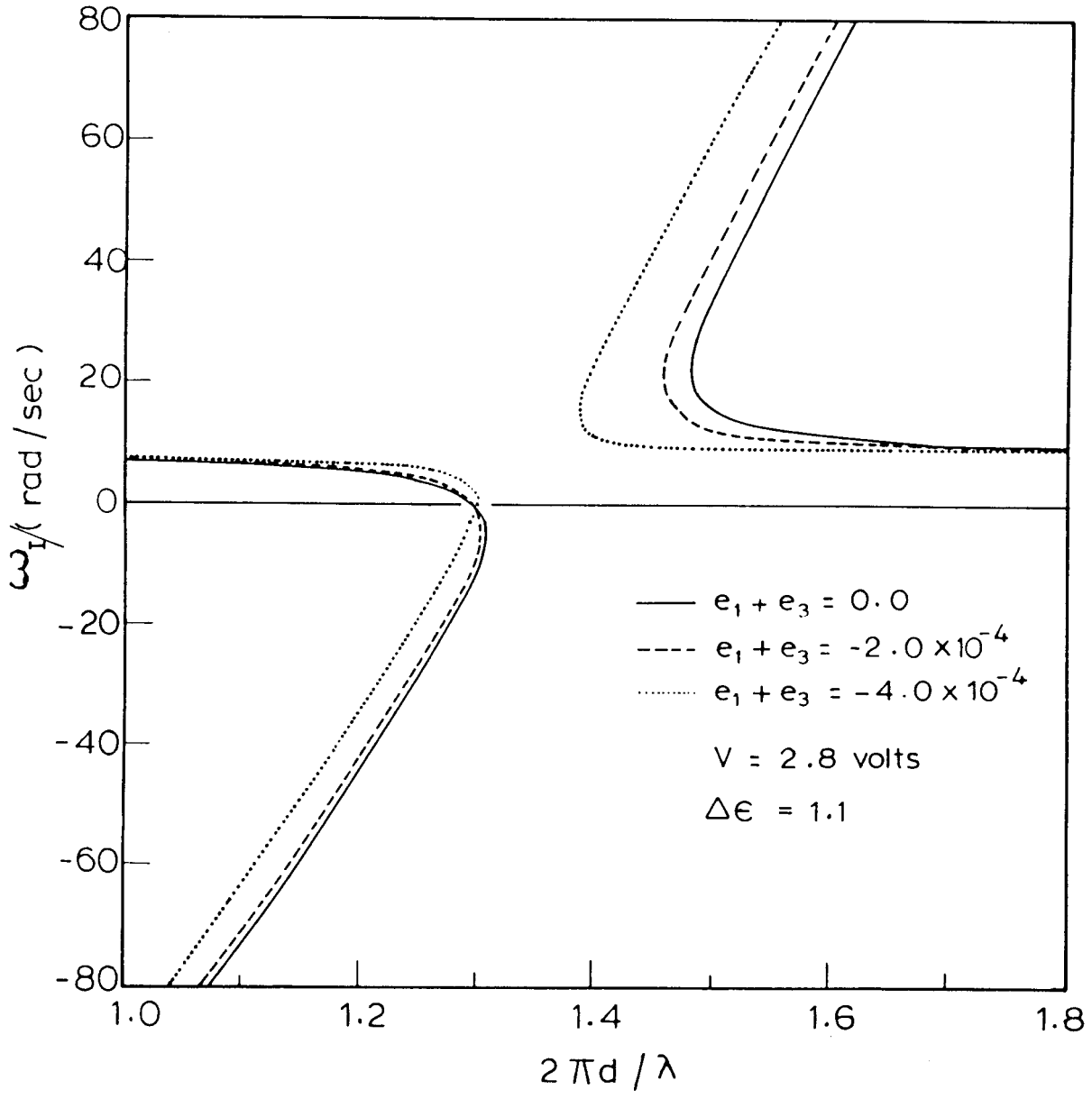

Fig.2.3: The calculated variation of ω_i with wavevector $q_x(2\pi d/\lambda)$. Note that the gap in the figure corresponding to oscillatory solutions decreases when the magnitude of $(e_1 + e_3)$ is increased.

Table 2.1

Material parameters of MBBA used in the calculations

$K_1 = 6.1 \times 10^{-7}$ dyne (1)	$\alpha_1 = 6.5$ cP (3)
$K_2 = 4.0 \times 10^{-7}$ dyne (2)	$\alpha_2 = -77$ cP (3)
$K_3 = 7.3 \times 10^{-7}$ dyne (1)	$\alpha_3 = -1.2$ cP (3)
$\epsilon_{\parallel} = 4.75$ (1)	$\alpha_4 = 83$ cP (3)
$\epsilon_{\perp} = 5.25$ (1)	$\alpha_5 = 46$ cP (3)
$\sigma_{\parallel} = 0.1 \times 10^{-10} \mathrm{ohm}^{-1}\mathrm{cm}^{-1}$	$\alpha_6 = -34$ cP
$\frac{\sigma_{\parallel}}{\sigma_{\perp}} = 1.5$ *(1)*	$(e_1 + e_3) = -7 \times 10^{-4}$ e.s.u. *(4)*
$\frac{\Delta\sigma}{\sigma_{\perp}} = 0.5$ (1)	$(e_1 - e_3) = 1 \times 10^{-4}$ e.s.u. (5)

1. Penz and Ford, 1972
2. Blinov, 1983
3. de Gennes, 1975
4. Madhusudana and Durand, 1985
5. Dozov *et al.*, 1982.

In order to understand the mechanism of the propagation mode, we first study the problem in a simple one-dimensional model, ignoring the boundary conditions. Figure 2.4 shows the geometry of the cell. We make the following simplifications:

1. The dielectric anisotropy of the medium is taken to be zero.

2. The pretilt angle β is assumed to be small (experimentally it is $\simeq 1-2°$) and hence we retain only linear terms in β.

3. We assume that the convective rolls are normal to $\hat{n}$, though the flexoelectric effect tends to produce oblique rolls under DC excitation (Madliusudana et al., 1987), and

4. From physical considerations (Helfrich, 1969; Orsay Liquid Crystal Group, 1970) q_x is set equal to π/d where d is the sample thickness.

Under these approximations, using the usual symbols, the linearised EHD equation can be written as -

1. The Poisson equation

$$4\pi Q - \epsilon\left(\frac{\partial E_x}{\partial x}\right) + 4\pi\beta(e_1+e_3)\frac{\partial^2\theta}{\partial x^2} = 0 \tag{2.20}$$

2. The charge continuity equation

$$\left(\frac{\partial Q}{\partial t}\right) + \sigma_{\|}\left(\frac{\partial E_x}{\partial x}\right) + \Delta\sigma E_o\left(\frac{\partial\theta}{\partial x}\right) = 0 \tag{2.21}$$

3. The torque balance equation

$$\gamma_1\left(\frac{\partial\theta}{\partial t}\right) + \alpha_2\left(\frac{\partial v_z}{\partial x}\right) - K_3\left[\frac{\partial^2\theta}{\partial x^2}\right] - \beta(e_1+e_3)\frac{\partial E_x}{\partial x} = 0 \tag{2.22}$$

4. The equation of motion along the Z-axis

$$\alpha_2\left(\frac{\partial^2\theta}{\partial x\partial t}\right) + \eta\left(\frac{\partial^2 v_z}{\partial x^2}\right) + E_o Q = 0 \tag{2.23}$$

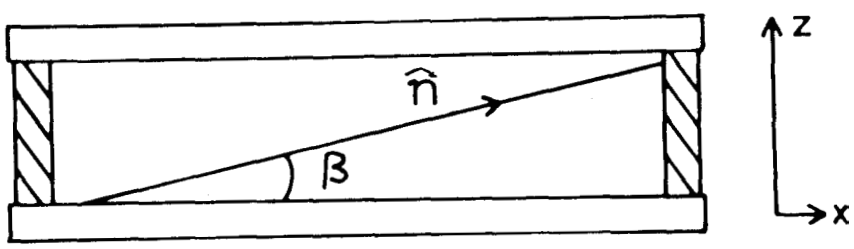

Fig.2.4: The experimental geometry for the propagating mode. β is the pretilt angle.

where $\eta = \dfrac{\alpha_4 + \alpha_5 - \alpha_2}{2}$

It is clear that under the approximations made in the present model, only the flexoelectric terms couple to the tilt angle. We again assume solutions of the following form.

$$\theta = \theta_1 e^{i(q_x x - \omega t)}; \qquad Q = Q_1 e^{i(q_x x - \omega t)}.$$
$$E_x = E_1 e^{i(q_x x - \omega t)} \quad \text{and} \quad v_z = v_1 e^{i(q_x x - \omega t)} \tag{2.24}$$

The amplitude equations corresponding to equations *(2.20)* to *(2.23)* are:

$$Q_1 - \frac{i\epsilon E_1 q_x}{4\pi} - \beta(e_1 + e_3)\theta_1 q_x^2 = 0 \tag{2.25}$$

$$Q_1\omega - \sigma_{\|} E_1 q_x - \Delta\sigma E_o \theta_1 q_x = 0 \tag{2.26}$$

$$(K_3 q_x^2 - i\gamma_1\omega)\theta_1 + iq_x\alpha_2 v_1 - iq_x\beta(e_1 + e_3)E_1 = 0 \tag{2.27}$$

and

$$E_o Q_1 + \alpha_2\omega q_x\theta_1 - \eta q_x^2 v_1 = 0 \tag{2.28}$$

Eliminating Q_1 from equations *(2.25)* and *(2.26)* we get,

$$E_1 = \left(\sigma_{\|} + \frac{i\epsilon\omega}{4\pi}\right)\frac{[\Delta\sigma E_o - \beta\omega(e_1 + e_3)q_x]}{(\sigma_{\|}^2 + \frac{\epsilon^2\omega^2}{16\pi^2})}\theta_1 \tag{2.29}$$

Eliminating v_1 from equations *(2.27)* and *(2.28)*

$$[\alpha_2\sigma_{\|}E_o - \omega\eta\beta(e_1 + e_3)q_x]E_1 + [-i\eta K_3\omega q_x^2 - \gamma_1\eta\omega^2 - \alpha_2^2\omega^2 + \alpha_2 E_o^2\Delta\sigma]\theta_1 = 0 \tag{2.30}$$

Now eliminating E_1 and θ_1 from equations *(2.29)* and (2.30), we get

$$\left(\sigma_{\|} + \frac{i\epsilon\omega}{4\pi}\right)[\Delta\sigma E_o - \beta\omega(e_1 + e_3)q_x][\alpha_2\sigma_{\|}E_o - \omega\eta\beta(e_1 + e_3)q_x] + [-i\eta\omega K_3 q_x^2 - r_1\eta\omega^2 - \alpha_2^2\omega^2 + \alpha_2 E_o^2\Delta\sigma]\left(\sigma_{\|}^2 + \frac{\epsilon^2\omega^2}{16\pi^2}\right) = 0 \tag{2.31}$$

The real part of the above equation leads to

$$4\pi K_3 q_x^2 + E_o^2 \epsilon \alpha_2 \left(\frac{\Delta\sigma}{\eta\sigma_{\|}}\right) - \frac{\epsilon\omega^2}{\sigma_{\|}}\left(\gamma_1 - \frac{\alpha_2^2}{\eta}\right) = 0 \tag{2.32}$$

From the imaginary part of equation (2.31) along with equation (2.32), we get

$$\omega = \frac{\beta(e_1 + e_3) q_x E_o (\frac{\Delta\sigma}{\sigma_{\|}} + \frac{\alpha_2}{\eta})}{(\gamma_1 - \frac{\alpha_2^2}{\eta})(1 + \frac{\tau}{T})} \tag{2.33}$$

where the charge relaxation frequency

$$\tau^{-1} = \frac{4\pi\sigma_{\|}}{\epsilon} \tag{2.34}$$

and tlie director relaxation frequency

$$T^{-1} = \frac{K_3 q_x^2}{(\gamma_1 - \frac{\alpha_2^2}{\eta})} \tag{2.35}$$

If $w = 0$, equation (2.32) reduces to the threshold condition obtained by Helfrich (1969) for the onset of stationary EHD instability. Further, since the third term in equation (2.32) has a negative sign, the propagating solution with a non-zero w has a ***lower*** threshold (E_o) than the threshold obtained for stationary instability with $\beta = 0$. The equation for w (2.33) contains tlie terrn E_o in it. In order to calculate E_o, we assume ω which is a small quantity to be zero. From equation (2.32) tlie threshold electric field becomes

$$E_o = \sqrt{\frac{-4\pi K_3 \eta \sigma_{\|}}{\epsilon \alpha_2 \Delta\sigma}}\, q_x \tag{2.36}$$

Now substituting for E_o from equation (2.36) in the equation (2.33), we calculate w and hence the velocity of propagation v.

$$\omega = \sqrt{\frac{4\pi K_3 \eta \sigma_{\|}}{\epsilon \alpha_2 \Delta\sigma}} \left[\frac{\beta(e_1 + e_3) q_x^2 (\frac{\Delta\sigma}{\sigma_{\|}} + \frac{\alpha_2}{\eta})}{(\gamma_1 - \frac{\alpha_2^2}{\eta})(1 + \frac{\tau}{T})}\right]$$

and

$$\mathbf{v} = \frac{\omega}{q_x} = \sqrt{\left(\frac{4\pi K_3 \eta \sigma_{\parallel}}{\epsilon \alpha_2 \Delta\sigma}\right)} \left[\frac{\beta(e_1 + e_3)\left(\frac{\Delta\sigma}{\sigma_{\parallel}} + \frac{\alpha_2}{\eta}\right)}{\left(\gamma_1 - \frac{\alpha_2^2}{\eta}\right)\left(1 + \frac{\tau}{T}\right)}\right] q_x \qquad (2.37)$$

From equation (2.37), we find that the velocity of propagation v is proportional to q_x. Further for a given sign of β and $(e_1 + e_3)$, the sign of w depends on the sign of E_o, i.e., the propagation reverses its direction when the applied electric field is reversed. As we have to assume $q_x = \frac{\pi}{d}$ in the one dimensional analysis, $\mathbf{v} \propto \frac{1}{d}$, i.e., velocity of propagation decreases in thicker samples.

The sum (e_1+e_3) of the flexoelectric coefficients arises from the aligned quadrupoles of the molecules and has a non-zero value in general (Prost and Mercerou, 1977). Therefore it is clear from equation (2.33) that the convective rolls obtained at the threshold of the instability should propagate normal to their axes. For the standard MBBA values of the material parameters (table 2.1) the velocity of propagation calculated using equation (2.37) is of the order of $0.1 \mu m/sec$.

The physical mechanism responsible for the propagating instability can be understood by referring to figure 2.5. The transverse electric field gradient in the medium is large in the region where the charge density is high. When $\beta = 0$ (Fig.2.5a) this cannot produce any torque on the quadrupoles of the medium. On the other hand, when $\beta \neq 0$ (Fig.2.5b), the field gradient produces a torque on the director. This torque is spatially $\pi/2$ radians out of phase with the torques produced by other physical mechanisms. Further, when $\beta \neq 0$, the flexoelectric polarisation has a divergence, which gives rise to space charge densities which are also $\pi/2$ radians out of phase with those collected by the coupling of the conductivity anisotropy with the curvature in the medium. The force produced by E_o on these additional charges gives rise to hydrodynamic torques, which are again $\pi/2$ radians out of phase with the main contributions responsible for the EHD instability. As a consequence

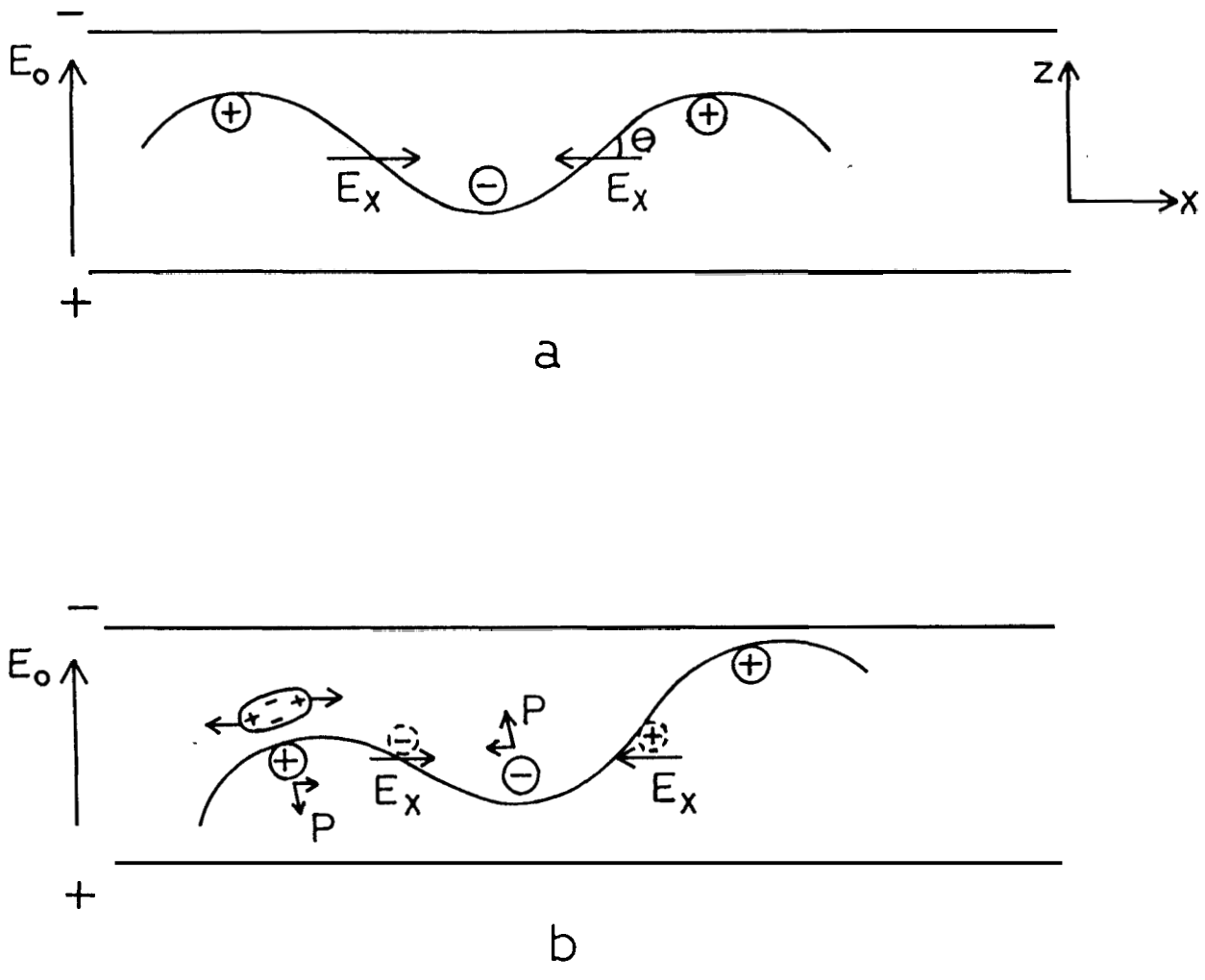

Fig.2.5: (a) β=0, the space charges (shown in full circles) arising from the conductivity anisotropy cause EHD instability. (b) When $\beta \neq 0$, the quadrupoles develop an out of phase torque due to the horizontal field gradients and additional charges (in dotted circles) are collected due to divergence of the flexoelectric polarisation $\vec{P}$.

of these out of phase torques, we get a slow propagation of the instability in the medium. Since the coupling responsible for the propagation is flexoelectric in origin, the direction of propagation depends on the sign of the applied field. Thus it is clear that this mechanism cannot explain travelling wave EHD instability which has been experimentally observed for AC fields (Rehberg *et* al., 1988, 1989).

2.4 Propagating EHD instability - two-dimensional calculations including the boundary conditions

We have confirmed the above result of the one-dimensional analysis by a more rigourous calculation using the appropriate boundary conditions. Under the same approximations made in one-dimensional calculations except for including the boundary conditions (see § 2.3), the linearised equations can be written as follows.

1. The Poisson equation

$$4\pi Q - \epsilon\left(\frac{\partial E_x}{\partial x}+\frac{\partial E_z}{\partial z}\right) - 4\pi(e_1+e_3)\frac{\partial^2\theta}{\partial x\cdot\partial z} + 4\pi\beta(e_1+e_3)\left(\frac{\partial^2\theta}{\partial x^2}-\frac{\partial^2\theta}{\partial z^2}\right)=0 \tag{2.38}$$

2. The charge conservation equation

$$\frac{\partial Q}{\partial t}+\sigma_{\parallel}\frac{\partial E_x}{\partial x}+\sigma_{\perp}\frac{\partial E_z}{\partial z}+\Delta\sigma E_o\frac{\partial\theta}{\partial x}+2\beta\Delta\sigma\left(\frac{\partial E_z}{\partial x}+E_o\frac{\partial\theta}{\partial z}\right)=0 \tag{2.39}$$

3. The torque balance equation

$$\gamma_1\frac{\partial\theta}{\partial t}-K_3\frac{\partial^2\theta}{\partial x^2}-K_1\frac{\partial^2\theta}{\partial z^2}+(e_1+e_3)\frac{\partial E_x}{\partial z}+\alpha_3\frac{\partial v_x}{\partial z}-\alpha_2\frac{\partial v_z}{\partial x}$$

$$+\beta\left[(e_1+e_3)\left(\frac{\partial E_z}{\partial z}-\frac{\partial E_x}{\partial x}\right)-2(K_1-K_3)\frac{\partial^2\theta}{\partial x\partial z}-2\gamma_2\frac{\partial v_x}{\partial x}\right]=0 \tag{2.40}$$

where $\gamma_2=(\alpha_2+\alpha_3)$

4. The equation of motion: x component

$$-\frac{\partial P}{dx} + \alpha_3 \frac{\mathbf{d^2 4}}{\mathbf{dzdt}} + \eta_1 \frac{\mathbf{d^2 v_x}}{\partial x^2} + \eta_2 \frac{\partial^2 v_x}{\partial z^2}$$

$$- \beta\left[\gamma_2 \frac{\partial^2 \theta}{\partial x \partial t} + \eta_5 \frac{\partial^2 v_z}{\partial z^2} - \eta_6 \frac{\partial^2 v_z}{\partial x^2}\right] = 0 \qquad (2.41)$$

where $\eta_1 = \left[\alpha_1 + \alpha_5 + \frac{\alpha_3 + \alpha_4 + \alpha_6}{2}\right]$; $\eta_2 = \left(\frac{\alpha_3 + \alpha_4 + \alpha_6}{2}\right)$;
$\eta_5 = (2\alpha_1 + 2\alpha_5 - \alpha_6)$ and $\eta_6 = \alpha_1 + \alpha_6$.

5. The equation of motion: z component

$$-\frac{\partial P}{\partial z} + \alpha_2 \frac{\partial^2 \theta}{\partial x \partial t} + \eta_4 \frac{\partial^2 v_z}{\partial x^2} + \eta_3 \frac{\partial^2 v_z}{\partial z^2} + E_o Q$$

$$+ \beta\left[\gamma_2 \frac{\partial^2 \theta}{\partial z \partial t} + \eta_7 \frac{\partial^2 v_x}{\partial x^2} + \alpha_6 \frac{\partial^2 v_x}{\partial z^2}\right] = 0 \qquad (2.42)$$

where $\eta_7 = (\alpha_1 + \alpha_6 - 2\alpha_5)$. In order to solve these equations we follow the same procedure outlined in section **2.2** of this chapter. Using solutions given by equation **(2.6)** in the above, we get the following amplitude equations

$$Q_1 - \frac{i}{4\pi} \epsilon q_x (s^2 + 1) E_1 + (e_1 + e_3) q_x^2 [(s^2 - 1)\beta + S]\theta_1 = 0 \qquad (2.43)$$

Substituting for Q_1 from equation **(2.43)** in equation **(2.39)** we get

$$E_1\left[S^2\left(\sigma_\perp + 2\beta\Delta\sigma - \frac{i\omega\epsilon}{4\pi}\right) + \sigma_\parallel - \frac{i\omega\epsilon}{4\pi}\right]$$
$$+ q_x[\{(S^2 - 1)\beta + S\}(e_1 + e_3)\omega + 2\beta\Delta\sigma U + \Delta\sigma U]\theta_1 = 0 \qquad (2.44)$$

$$E_1[\beta(S^2 - 1) + S]i(e_1 + e_3) + \theta_1\left[K_1 q_x S^2 + 2\beta(K_3 - K_1) q_x S + K_3 q_x - \frac{i\omega\gamma_1}{q_x}\right]$$
$$- iv_1[\alpha_3 S^2 - 2\gamma_2 S - \alpha_2] = 0 \qquad (2.45)$$

$$iP_1 - \theta_1(\alpha_3 S - \gamma_2\beta)\omega - v_1(\eta_2 S^3 + \eta_5 \beta S^2 + \eta_1 S - \eta_6\beta) q_x = 0 \qquad (2.46)$$

$$- \quad iSP_1 + \theta_1[-U(e_1+e_3)q_x^2\left\{\beta(S^2+1)+S\right\} + (\gamma_2\beta S + \alpha_2)\omega]$$
$$+v_1[\alpha_6\beta S^3 - \eta_3 S^2 + \eta_7\beta S - \eta_4] + \frac{iU\epsilon}{4\pi}(S^2+1)q_x E_1 = 0 \qquad (2.47)$$

Eliminating P_1 from the equations (2.46) and (2.47)) we get

$$E_1\frac{iU\epsilon}{4\pi}q_x(S^2 + 1) + \theta_1[-\{\alpha_3\omega + U(e_1+e_3)q_x^2\beta\}S^2 + \{2\gamma_2\beta\omega - U(e_1+e_3)q_x^2\}S$$
$$+ \alpha_2\omega - U(e_1+e_3)\beta q_x^2] + v_1[-\eta_2 S^4 + (\alpha_6 - \eta_5)\beta S^3$$
$$- (\eta_1+\eta_3)S^2 + (\eta_6+\eta_7)\beta S + \eta_6\beta - \eta_4] = 0 \qquad (2.48)$$

For the existence of non-trivial solutions the determinant of the coefficients of variables, namely E_1, v_1 and θ_1 in the equations (2.44), (2.45) and (2.48) should vanish

$$\begin{bmatrix} (A_1S^2 + A_2) & 0 & (A_3S^2 + A_4S + A_5) \\ (B_1S^2 + B_2S - B_1) & (B_6S^2 + B_7S + B_8) & (B_3S^2 + B_4S + B_5) \\ (C_9S^2 + C_9) & (C_4S^4 + C_5S^3 + C_6S^2 + C_7S + C_8) & (C_1S^2 + C_2S + C_3) \end{bmatrix} = 0 \qquad (2.49)$$

where

$A_1 = (\sigma_\perp + 2\beta\Delta\sigma - \frac{i\omega\epsilon}{4\pi})$; $A_2 = \sigma_\parallel - \frac{\text{iwc}}{4\pi}$; $A_3 = (e_1 + e_3)\omega\beta q_x$;

$A_4 = A_3/\beta$; $A_5 = -A_4 + 2\beta\Delta\sigma U + \Delta\sigma U$; $B_1 = i\beta(e_1+e_3)$;

$B_2 = i(e_1+e_3)$; $B_3 = K_1 q_x$; $B_4 = 2\beta(K_3 - K_1)q_x$;

$B_5 = K_3 q_x - \frac{i\omega\gamma_1}{q_x}$; $B_6 = -i\alpha_3$; $B_7 = 2i\gamma_2$ $B_8 = i\alpha_2$;

$C_1 = -\{\alpha_3\omega + U(e_1+e_3)\beta q_x^2\}$; $C_2 = 2\gamma_1\beta\omega - U(e_1+e_3)q_x^2$;

$C_3 = \alpha_2\omega - U(e_1+e_3)\beta q_x^2$; $C_4 = -\eta_2$; $C_5 = (\alpha_6 - \eta_5)\beta$;

$C_6 = -(\eta_1+\eta_3)$; $C_7 = (\eta_6+\eta_7)\beta$; $C_8 = \eta_6\beta - \eta_4$; $C_9 = \frac{iUe}{4\pi}q_x$

Equation (2.49) yields the following 8th degree polynomial in S

$$\sum_{j=0}^{8} a_j S^j = 0 \qquad (2.50)$$

where S^j is the j^{th} power of S and a_j is the corresponding coefficient. The roots of equation (2.50) can be determined using the eight boundary conditions that tlie variables θ, E_x, v_x and v_z have to satisfy at tlie two surfaces of the cell. These boundary conditions are

$$\theta(z = \pm d/2) = \beta, \text{the pretilt angle;} \quad E_x(z = \pm d/2) = 0;$$
$$v_x(z = \pm d/2) = 0 \quad v_z(z = \pm d/2) = 0 \tag{2.51}$$

As before, using these boundary conditions we write the boundary value determinant (BVD)

$$D_{ij} = 0; i, j = 1, 8 \tag{2.52}$$

This boundary value problem was solved by the method used in section (2.2) of this chapter.

Using the standard MBBA values of the material parameters, we have calculated tlie threshold voltage and the frequency w as functions of tlie pre-tilt angle β (Fig.2.6). For the range of β values shown, the wavevector q, $\approx 4/d$. The linear variation of w with β is in agreement with the prediction of the one-dimensional model, viz., equation (2.33). The threshold voltage is also almost independent of β which is assumed to be small. Further the direction of propagation is found to depend upon the signs of the applied electric field E,, the pretilt angle β and the sign of $(e_1 + e_3)$.

2.5 Experimental

2.5.1 Construction of the cell

The cell is made of two indium tin oxide coated glass plates with their conducting surfaces treated with polyimide. The plates are rubbed unidirectionally and a sand-

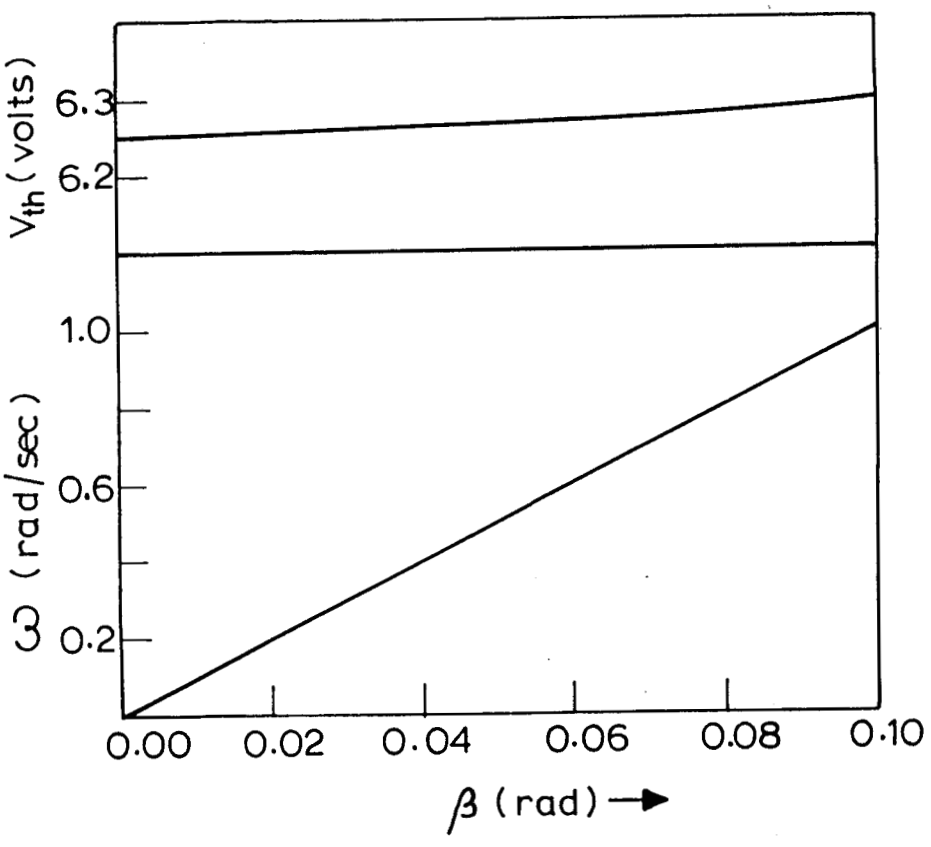

Fig.2.6: Variation of V_{th} and w with pretilt angle β obtained from calculations including the boundary conditions. $\Delta\epsilon$=0 and other material parameters have the MBBA values at **303** K. Thickness of the cell = 15 μm.

wich cell is prepared by placing two such glass plates with their rubbing directions opposing each other (Fig.2.7). Mylar spacers are used between the glass plates to control the thickness of the cell which is sealed at the edges using an epoxy compound. The cell is filled with a room temperature nematic liquid crystal mixture, whose composition is described later in this section. If a standard 3% polyimide solution is used to get the alignment, the EHD patterns obtained under DC *excitation* are rather patchy and further the threshold varied considerably with time. Presumably a dense coating of polyimide acts as an insulating layer which reduces the field in the sample as ions collect near these layers (see Blinov, 1983). However on reducing the concentration of the polyimide to about 1/20th of the standard value, we get better EHD pattern under DC excitation. This is probably due to a porous coating of the polymer. The alignment obtained under these conditions remain satisfactory.

The cell thickness is measured using an optical interferometric technique. The light reflected normally from the two glass surfaces bounding the air gap corresponding to the cell thickness is made to fall on a constant deviation spectroscope (Adam and Hilger Ltd.). A spectrum with alternate dark and bright fringes is seen due to interference of light reflected from the two surfaces of the cell forming the air film. The cell thickness is calculated using the expression,

$$d = \left(\frac{\lambda_m \times \lambda_n}{\lambda_m - \lambda_n}\right) \times \left(\frac{n-m}{2}\right)$$

where λ_m and λ_n are the wavelengths corresponding to m^{th} and n^{th} dark fringes respectively.

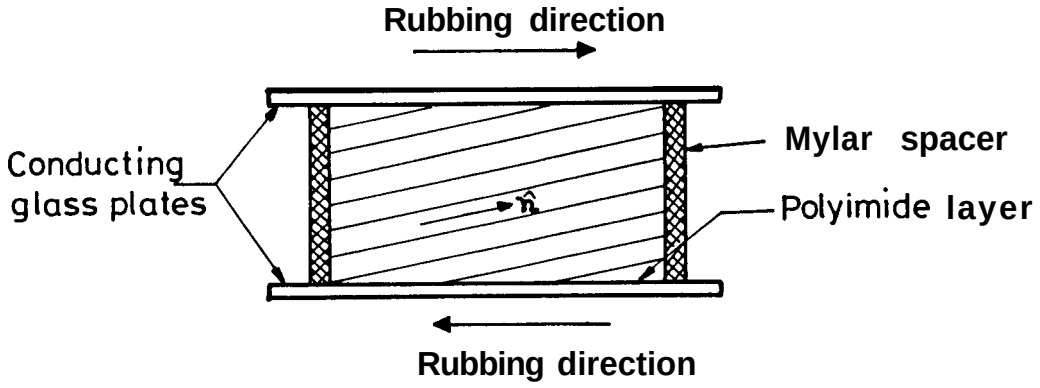

Fig.2.7: The cross-section of the cell with the antiparallel arrangement of unidirectionally rubbed polyimide coated glass plates. The nematic director $\hat{n}$ though tilted is uniformly aligned in the cell.

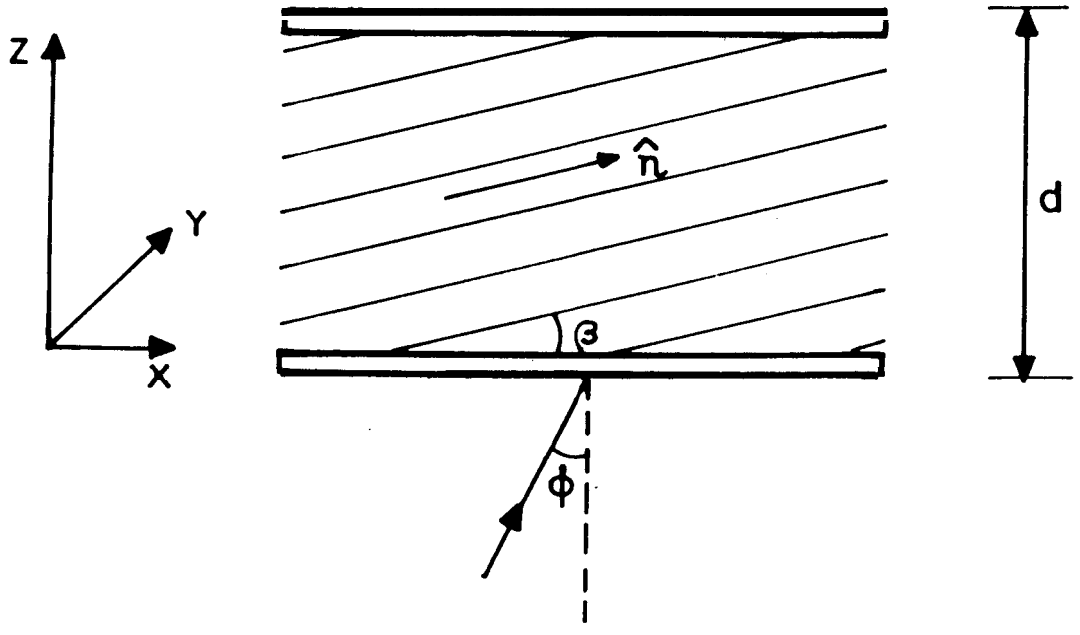

Fig.2.8: Cross section of a liquid crystal cell showing the pretilt angle β and ϕ the angle of incidence of the light beam.

2.5.2 Measurement of pre-tilt angle

To measure the low pre-tilt angle accurately we have used the crystal-rotation method (Baur et al., 1976 and Nakano et al., 1980).

The NLC is confined between the cell plates, whose rubbing directions are antiparallel. We have then a uniaxial medium with its optic axis at an angle β with respect to the plane of the plates (Fig.2.8). Let ϕ be the angle of incidence of the light beam. Then the nematic director $\hat{n}$ and the wave normal $\vec{S}$ of the incident beam is defined by the vectors,

$$\begin{aligned} \hat{n} &= (\cos\beta, 0, \sin\beta) \qquad 0^o \leq \beta \leq 90^o \\ \mathrm{S} &= (\sin\phi, 0, \cos\phi) \qquad -90'' \leq \phi \leq 90'' \end{aligned}$$

The transmission of light through such a uniaxial medium placed between parallel polarisers and with the plane of polarisation of the incident light making an angle of 45" with the projection of the director on cell walls, is given by (Nakano et al., 1980)

$$T(\phi) = \cos^2\left[\frac{\pi d}{\lambda}\left(\frac{n_o n_e\sqrt{n^2(\beta) - \sin^2\phi}}{n^2(\beta)} - \frac{n_e^2 - n_o^2}{n^2(\beta)}\sin\beta\cos\beta\sin\phi\right)\right] \qquad \textbf{(2.53)}$$

where λ is the wavelength of the incident radiation, n_o and n_e are the ordinary and extraordinary refractive indices of the nematic liquid crystal respectively, and

$$n(\beta) = \sqrt{n_o^2\cos^2\beta + n_e^2\sin^2\beta} \qquad \textbf{(2.54)}$$

The intensity vs. ϕ curve obtained from equation (2.53) for typical values of n_e, n_o are given in figure 2.9. Equation (2.53) is differentiated to get the followirig condition for minimum in the intensity of transmitted liglit

$$\left[(n_o^2 - \sin^2\phi_x)^{-1/2} - \frac{n_o n_e}{n^2(\beta)}\left(n^2(\beta) - \sin^2\phi_x\right)^{-1/2}\right]\sin\phi_x = \frac{n_e^2 - n_o^2}{n^2(\beta)}\sin\beta\cos\beta \qquad (2.55)$$

Assuming that β is very small, equation (2.55) can be approximated as follows,

$$\sin 2\beta = \frac{-2\sin\phi_x}{(\mathrm{no} + n_e)\sqrt{1 - (\sin\phi_x/n_o)^2}} \qquad (2.56)$$

This minimum corresponds to that shown by the dotted line about which the interference pattern is approximately symmetric (Fig.2.9).

In the experiment, the angle ϕ is measured using a goniometer spectrometer (Freiberger). The cell is mounted vertically on the prism table, such that the plane of the cell is at right angles to the plane of the prism table. The cell is rotated about an axis which is perpendicular to the rubbing direction (Fig.2.10). We have used the CGS units in all the theoretical calculations though presenting our experimental results we have consistently used the S.I. units. The incident light from a sodiurn source is passed through the collimator and is polarised at an angle of 45° with respect to the rubbing direction. The light intensity is measured using a photodiode (Centronics). ϕ is varied from +60° to -60°. The transmitted intensity is plotted against the angle of incidence in figure 2.11. From the graph, the angle ϕ_x at which the transmittance curve has a minimum is noted. Then from equation (2.56) the pretilt angle β is calculated.

We used a room temperature nematic liquid crystalline mixture consisting of 46 mole % (2-methylphenyl)-bis-4-n-butylbenzoate (RO-CE 1700), 50 rnole % 1-n-propyl-4[4-ethoxyphenyl]-cyclohexane (PCH-302) and 4 mole % 4'-n-pentyl-4-cyano-

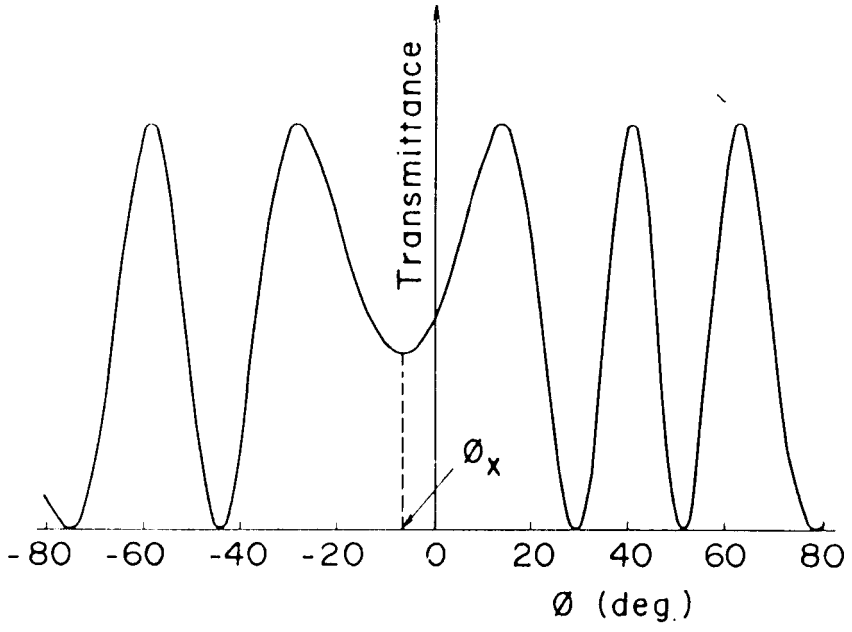

Fig.2.9: Angular dependence of intensity of transmitted light (Ref. Nakano *et al:*, 1980).

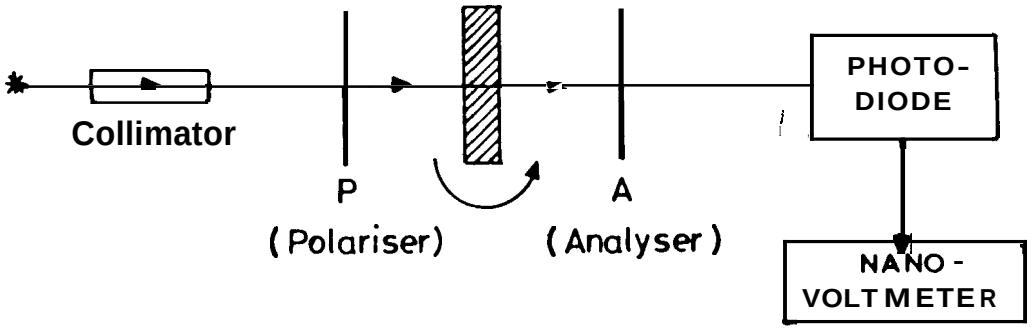

Fig.2.10: Schematic representation of the experimental set up used to measure tilt angles.

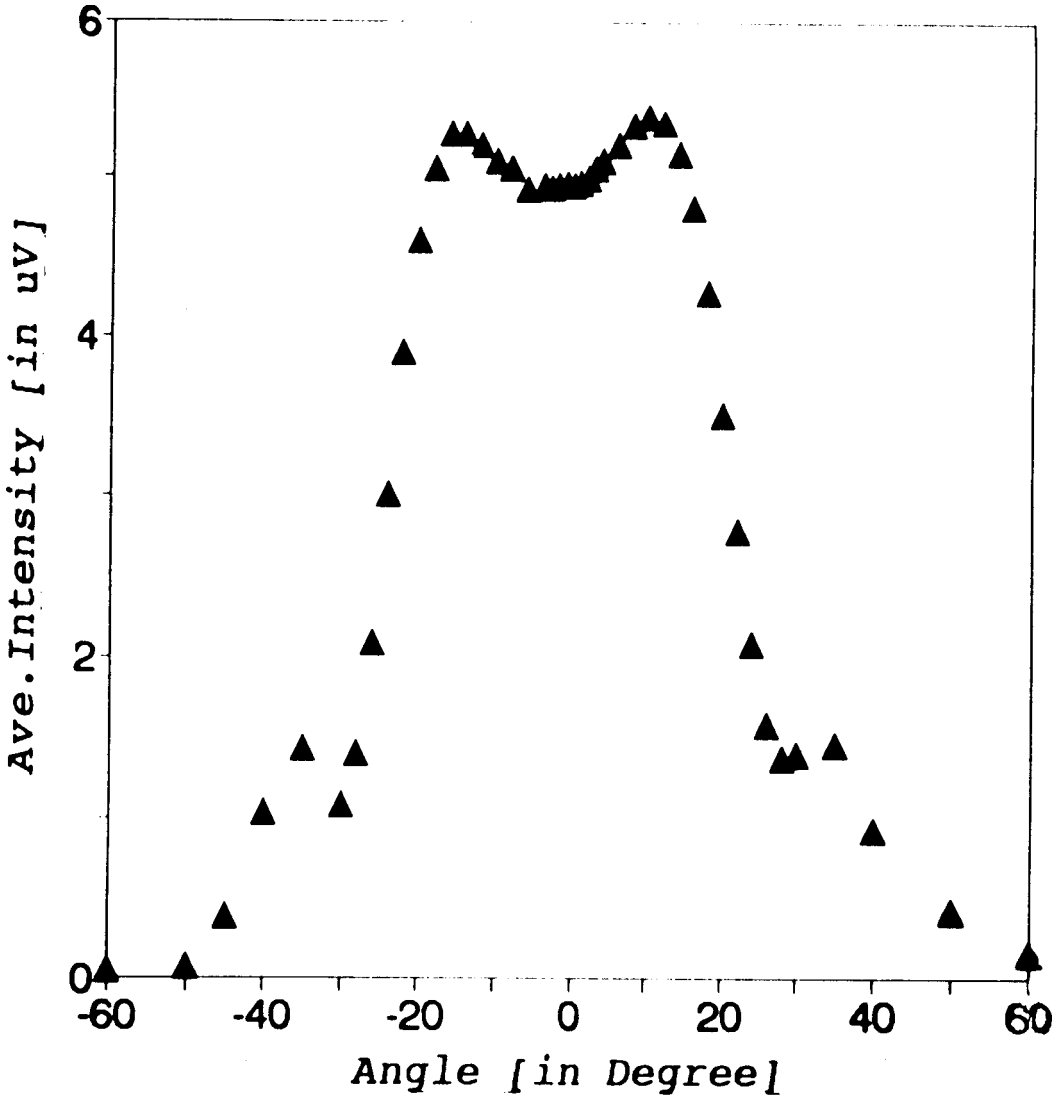

Fig.2.11: Angular dependence of transmitted light intensity (λ=5893 x $10^{-10}m$) for a cell of tliickness 53.0 μm for nematic liquid crystal mixture with n_o=1.501 and n_e=1.639 at room temperature. The value of β=1.2°.

biphenyl (5CB). These are commercial compounds obtained from Hoffman La Roche and are chemically stable. The structural formulae and transition temperatures of these compounds are given in figure 2.12. This mixture has a low negative dielectric anisotropy. We have also added about 0.1% of ionic impurities such as tetrabutylammonium bromide (TBAB), to increase the conductivity of the mixture to about 10^{-7} ohm $^{-1}$ m^{-1}. The refractive indices n_o and n_e of this mixture were measured by an independent experiment using an Abbe refractometer. The values obtained were $n_o = 1.501$ and $n_e = 1.639$. For the cell used in our experiment β was found to be 1.2".

2.5.3 Experimental study of propagating mode

For observing the propagating EHD instabilities, the liquid crystal cell is mounted on the stage of a Leitz polarising microscope (Orthoplan). A Mettler hot stage (FP82) is used to regulate the temperature of the cell. At room temperature the pattern observed at the threshold under DC excitation consisted of propagating oblique rolls whose propagation direction reversed when the field was reversed. On increasing the temperature, the obliquity of the rolls decreased and at about 333 K almost normal rolls were obtained. In order to minimise the influence of the moving boundaries between domains of opposite tilts of the rolls on the propagation of the rolls themselves, we have made all the detailed observations at about 333 K. Preliminary video-prints (Fig.2.13) clearly show the propagating modes. In order to make more quantitative measurements we used better samples and the EHD pattern is recorded using a CCD video camera (Sony) mounted on the microscope. The video output, which is digitised with a resolution of 512 x 512 pixels of 256 grey levels, is fed to an IBM Personal Computer with a frame grabber (Fig.2.14). The frame

RO – CE 1700

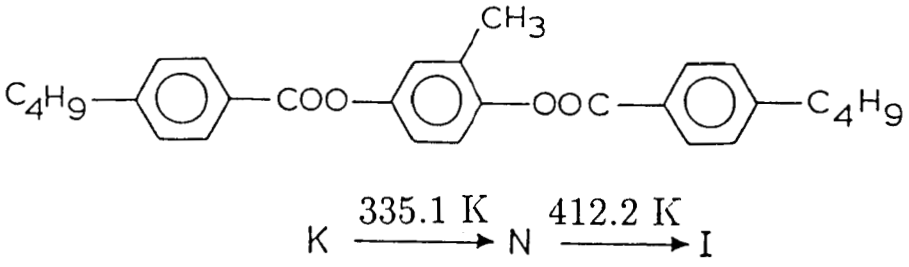

PCH 302

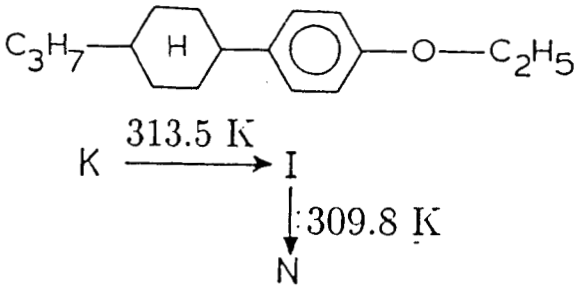

5 CB

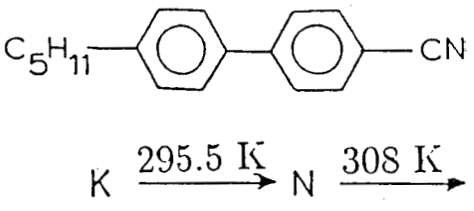

Fig.2.12: Structural formulae and transition temperature of the compounds used in the mixture.

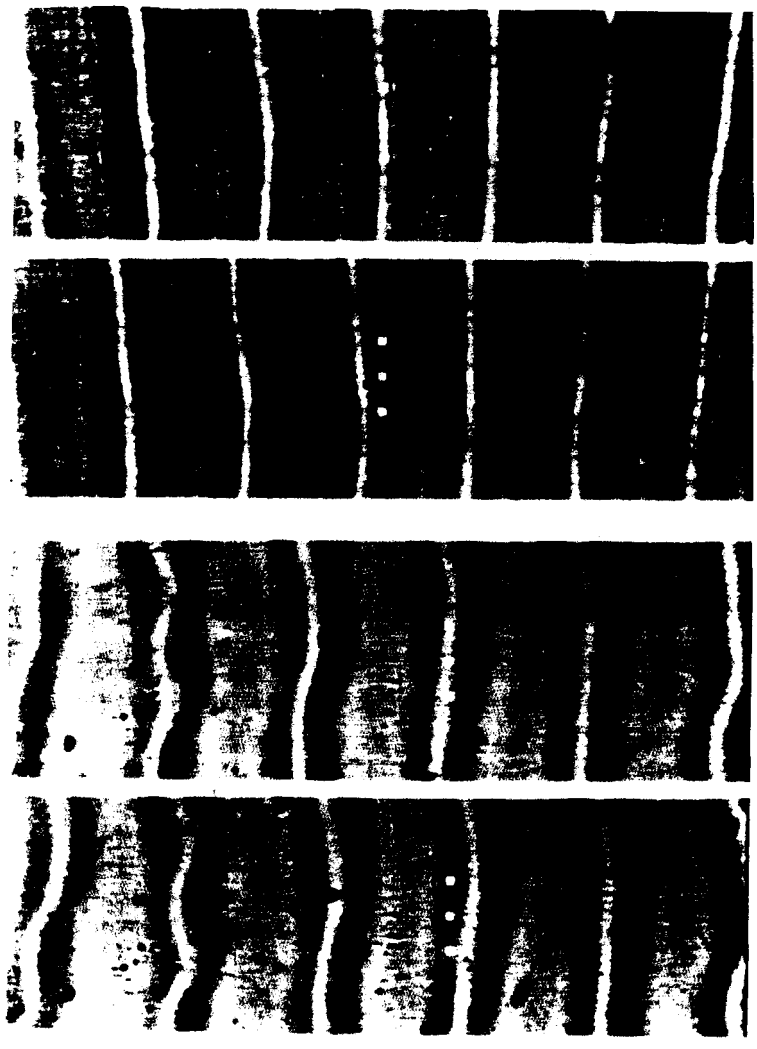

Fig.2.13: Video prints of propagating electroconvection in a nematic mixture under DC excitation in a cell of d=80 μm. Starting from the top, the video recordings correspond to (i) t = 0, (ii) t = 120 sec. for V_z = \$2.4 V, (iii) t = 0 and t = 120 sec. for V_z=-2.4V. Each optical domain contains two rolls of opposite vorticity. The sensitivity of the DC instability to local surface conditions causes the deviations from straight rolls. (magnification x 70).

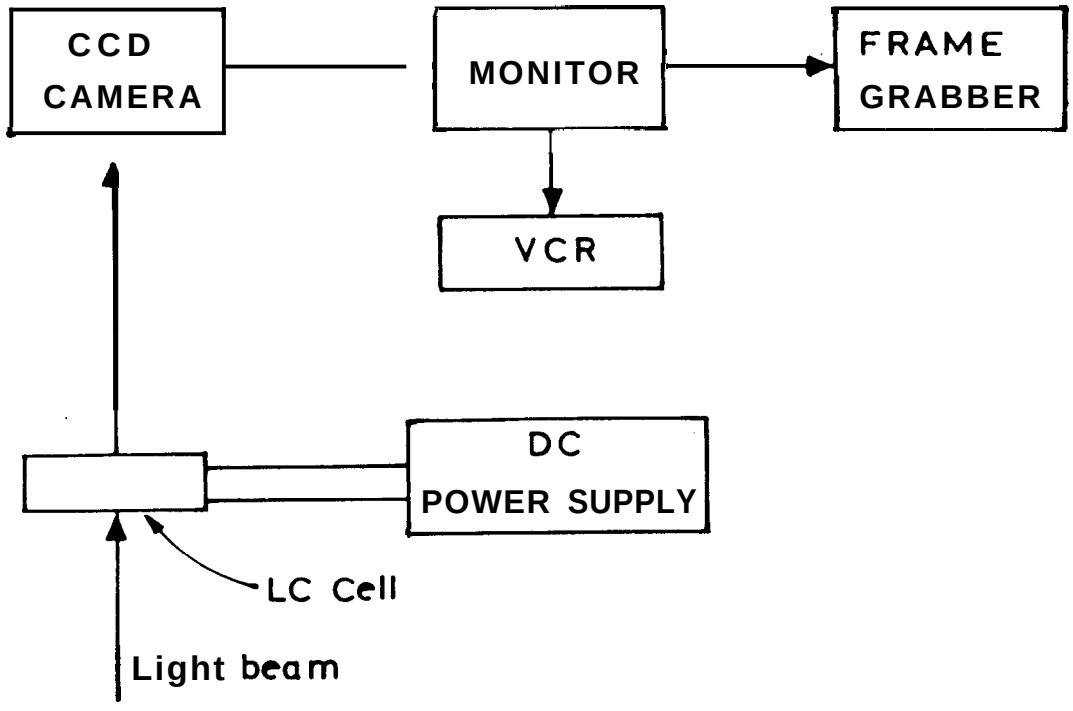

Fig.2.14: Schematic representation of the experimental set-up used to observe propagating EHD instability.

grabber is programmed to grab a video frame at intervals of 2 sec. Then successive intensity profiles along a line normal to the roll axis are sequentially plotted as shown in figure 2.15. In the absence of any propagation the line joining tlie peaks of the successive profiles would remain vertical. But when there is propagation of domains, the line joining tlie intensity peaks form an angle with the vertical as shown in figure 2.15. With the reversal of the applied field, this line takes the opposite slope indicating the reversal of the direction of propagation of EHD pattern.

In order to illustrate the phenomenon and also bring out the problems connected with a DC experiment, we first describe the results on a cell of thickness 17.5 μm at 333 K. The velocity of propagation is also found to be sornewhat different for tlie two signs of the voltage,viz., $0.9\mu m/sec$ for positive voltage slightly above threshold and $-0.5\mu m/sec$ for negative voltage. Under AC excitation the EHD pattern was found to drift with a velocity of about $+0.2\ \mu m/sec$ just above the threshold. Hence the difference in the propagating velocity for positive and negative voltages could arise from a small thickness gradient present in the cell which leads to a drift of the pattern in a particular direction independent of the sign of the voltage. We have also observed that the threshold voltages are slightly different for positive and negative applied voltages (Fig.2.16). This is probably due to some assymmetry in the coating on the two electrodes.

We have also studied the thickness dependence of tlie velocity of the propagating mode (Fig.2.17). The velocities measured using two cells of thickness 12.7 μm and 53.0 μm are 1.4 $\mu m/sec$ and 0.5 $\mu m/sec$ respcctivcly at 333 K. The velocity approximately goes as $1/d$. In view of the inherent problems associated with DC fields, the errors in these mcasurcments are relatively high. From figure 2.6 wc scc that for a pretilt of 1.2" the propagation velocity obtained from the theory for $\Delta\epsilon = 0$

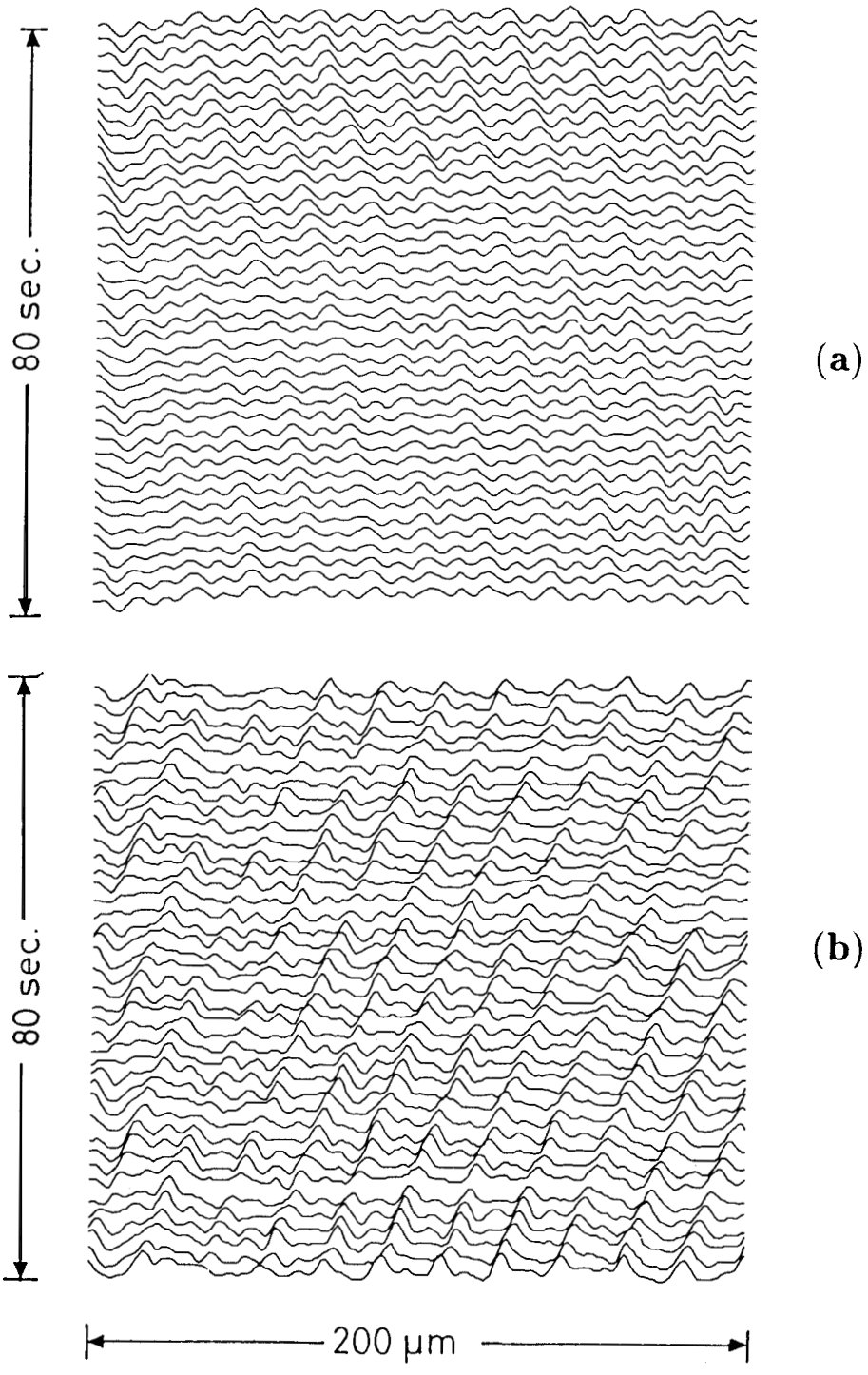

Fig.2.15: The light intensity profiles along a line normal to the rolls recorded at intervals of 2 secs. plotted on top of one another. (a) V=-8.9 volt , (b) V=+8.9 volt (V_{th}=8.5 volt). Note that tlie rolls propagate in opposite directions for opposite signs of the voltage. Thickness of the cell = 15 μm, temperature = 333 K.

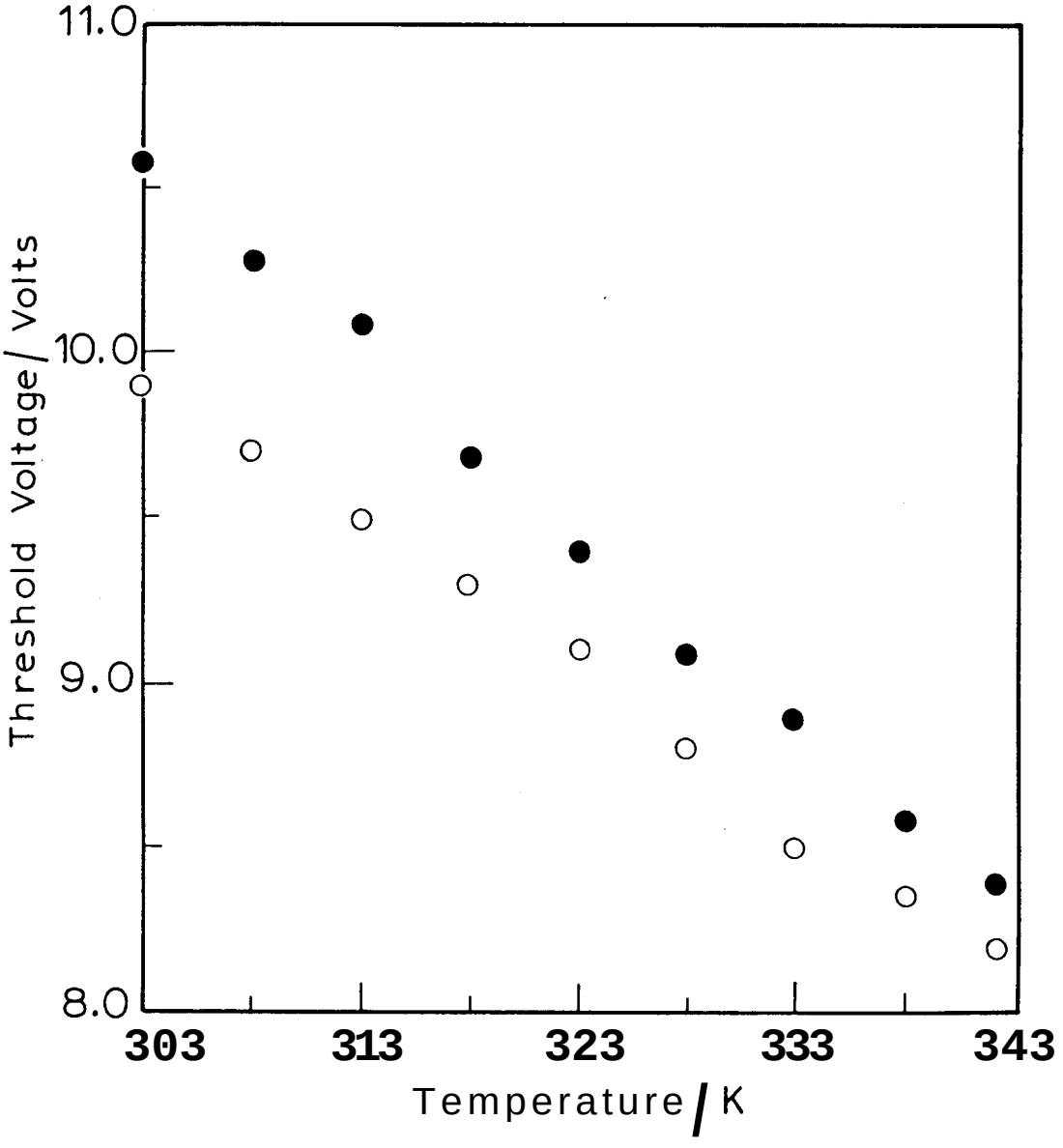

Fig.2.16: Variation of threshold voltage with temperature for a cell of d=17.5 μm, filled with nematic liquid crystal mixture with T_{NI}=342.8 K. ● for negative field and ○ for positive field. It may be noted here that the EHD pattern consists of oblique rolls below the temperature 333 K.

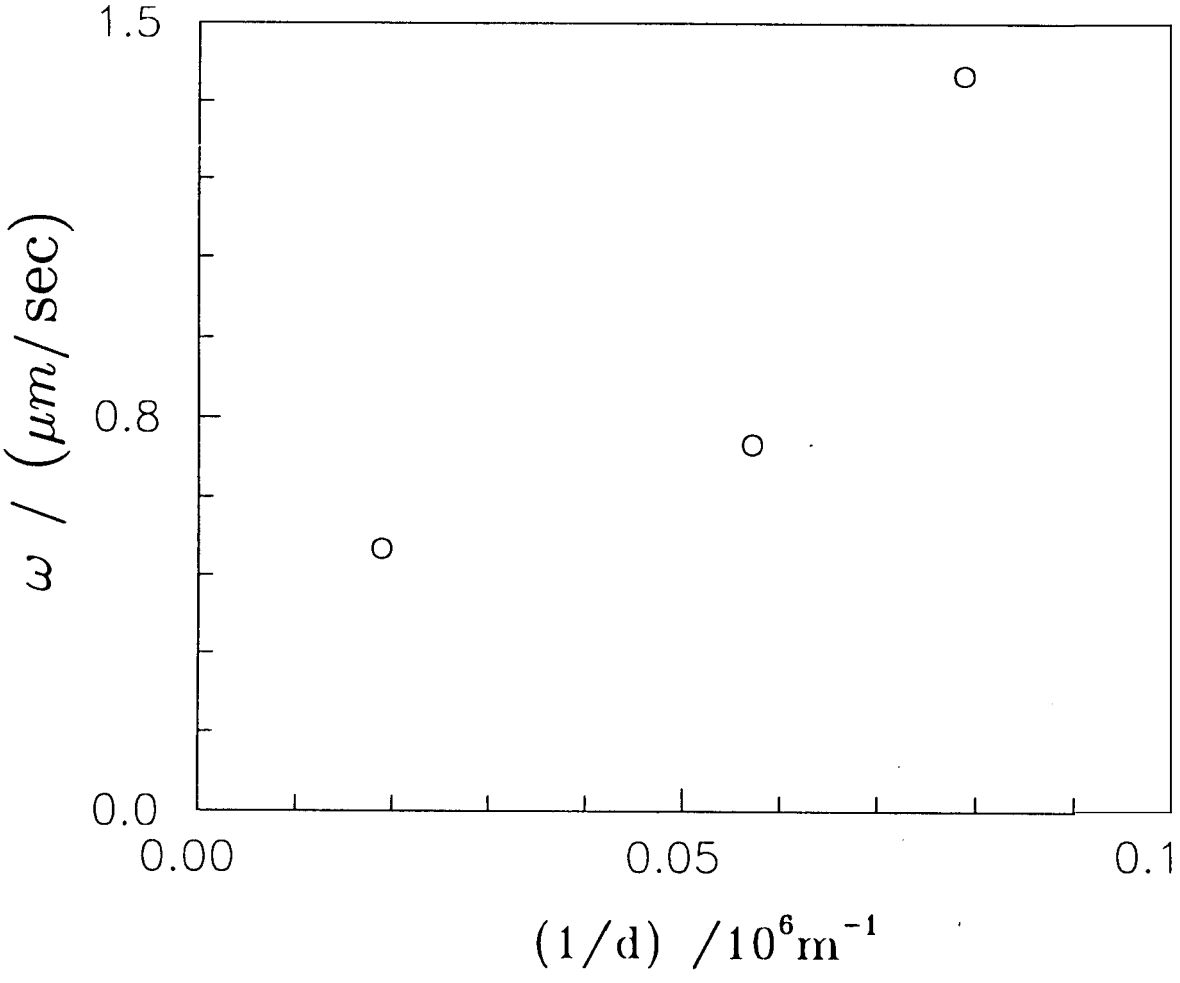

Fig.2.17: Thickness dependence of velocity of propagating modes at temperature **333** K.

and for MBBA values of other material parameters at 303 K is about 0.5 $\mu m/sec$ for a cell with d=15 μm. Thus the observed propagation velocity is comparable to that obtained from the theory. We have determined the sign of $(e_1 + e_3)$ for this mixture to be negative (see Chapter IV). For the experimental configuration used (Fig.2.5), the theory predicts that the direction of propagation is along the positive X-axis for positive E_o. This direction agrees with the observations (taking into account the image inversion in the microscope).

We have repeated these experiments at different temperatures, and made the following observations. The threshold voltage decreases with increase in temperature (Fig.2.16) whereas the velocity of propagation increases with increase in temperature (Fig.2.18). From the equation for threshold field (eqn.2.36) it is clear that the decrease of threshold voltage is due to the decrease of K_3 with temperature. From equation (2.37), velocity of propagation is $\propto \frac{1}{\gamma}$. Therefore the velocity of propagation is expected to decrease with increase of temperature.

2.6 Conclusion

The oscillatory solutions of the EHD equations which were found by Penz to exist over a narrow voltage range above the Freedericksz threshold for a nematic with positive $\Delta\epsilon$ in a planar aligned cells are suppressed by the flexoelectric effect. However if the nematic is aligned with a small pretilt of the director at the bounding surfaces, the flexoelectricity of the medium leads to a propagating EHD instability under DC excitation. The results of our experiments on the propagating instability are in qualitative agreement with the theoretical predictions.

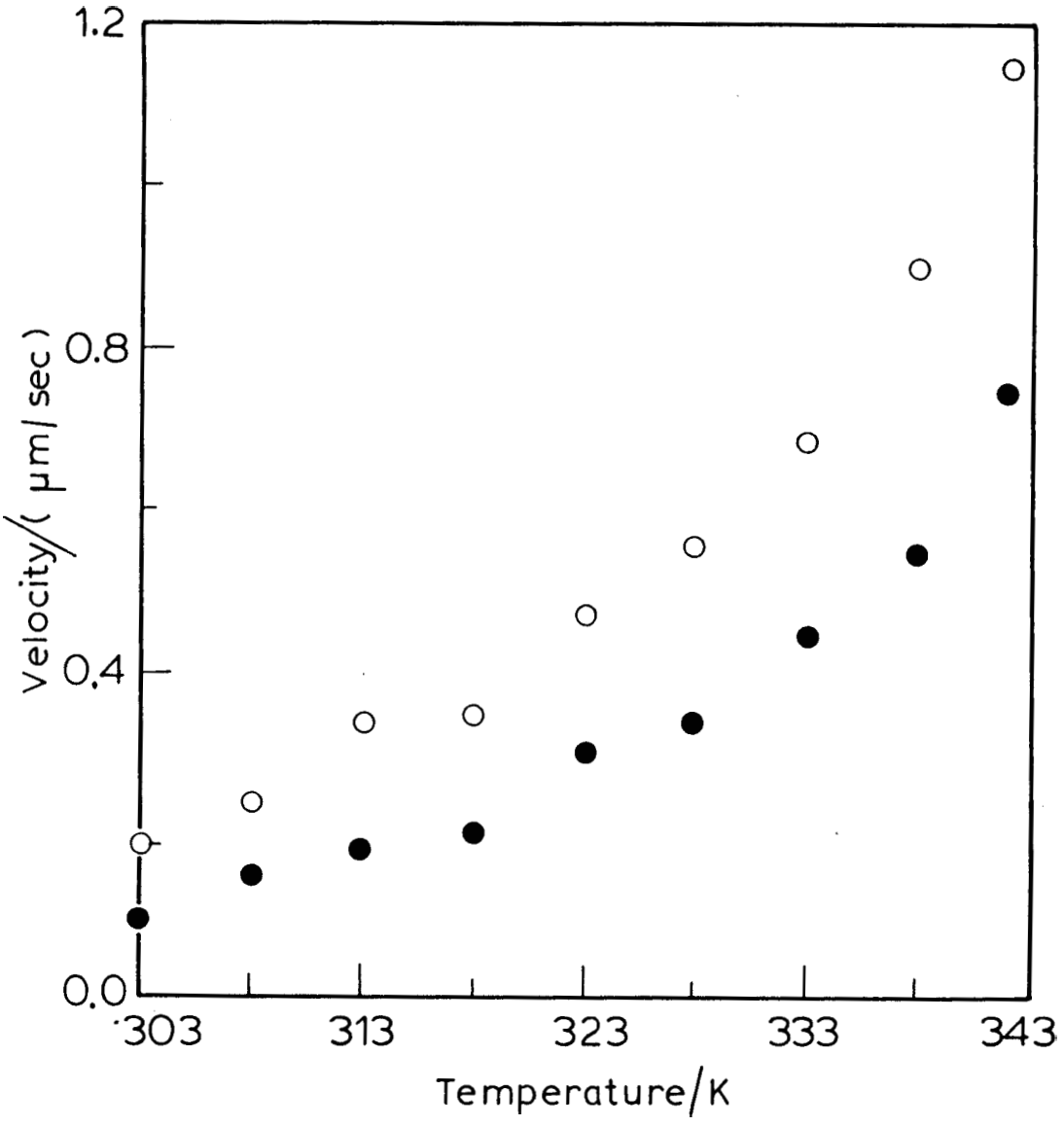

Fig.2.18: Variation of the velocity of propagating mode with temperature for a cell of d=17.5 μm, filled with NLC mixture with T_{NI}=342.8 K ● for negative field and ○ for positive field. In all these observations the dimensionless ratio $\epsilon = \frac{V-V_{th}}{V}$ is maintained at a value <0.05. The EHD pattern consists of ohliquc rolls below the temperature **333** K.

References

BAUR,G., WITTEWER,V., and BERREMANN,D.W., 1976, Phys. Letters, **56A**, 142.

BLINOV,L.M., 1'383, *Electro-optical* and Magneto-optical l'roperties of Liquid Crystals, (Wiley, New York).

DE GENNES, P.G., 1975, The Physics of Liquid Crystals (Clarendon, Oxford).

DOZOV,I., MARTINOT-LAGARDE,Ph., and DURAND,G., 1982, J. de Phys., 43, L365.

HELFRICH,W.J., 1969, J. Chem. Phys., 51, 4092.

IOFFE,I.V., 1975 *Sov.* Phys. Tech. Phys., 19, 1012.

KRAMER,L., BODENSCHATZ,E., PERCH,W., THOM,W., and ZIMMERMANN,W., 1989, Liquid Crystals, 5, 699.

LAIDLAW,W.G., 1979, Phys. Rev., A20, 2188.

LEKKERKERKER,H.N.W., 1978, J. *Phys.* (Paris) Lett., 38, 277.

LOWE,M., and GOLLUB,J.P., 1985, *Phys.* Rev. Lett., 55, 2.575.

MADHUSUDANA,N.V. and DURAND,G., 1985, J. de Phys., 46, L195.

MADHUSUDANA,N.V., RAGHUNATHAN,V.A., and SUMATHY,K.R., 1987, Pramana - J. Phys., 28, L-311.

MADHUSUDANA,N.V., and RAGHUNATHAN,V.A., 1989, Liquid Crystals, 5, 1789.

MATYUSHICHEV,Yu, and KOVNATSKII,A.M., 1975, *Sov.*Phys. Tech.Phys., 20, 409.

MOSLEY,A., NICHOLAS,B.M., and GASS,P.A., 1987, Displays, **8,** 17.

NAKANO,F., ISOGAI,M., and SATO,M., 1980, Japan **J.** *Appl. Phys.*, **19,** 2013.

ORSAY LIQUID CRYSTAL GROUP, 1970, Phys. Rev. Lett., 25, 1642.

PENZ,P.A., 1975, Phys. Rev., A12, 1585.

PENZ,P.A., and FORD,G.W., 1972, *Phys.* Rev., A6, 414.

PROST,J., and MARCEROU,J.P., 1977, **J.** de Phys., 38, 315.

RAGHUNATHAN,V.A., MAHESWARA MURTHY,P.R., and MADHUSUDANA,N.V., 1990, Current Science, 59, 506.

REHBERG,I., RASENAT,S., FINEBERG,J., DE LA TORRE JUAREZ,M., and STEINBERG,V., 1988, *Phys. Rev.* Lett., 61, 2449.

REHBERG,I., RASENAT,S., and STEINBERG,V., 1989, Phys. Rev. Lett., 62, 756.

THOM,W., ZIMMERMANN,W., and KRAMER,L., 1989, Liquid Crystals, 4, 309.